# ARTICLES

## Optical and Field Emission Properties of Thin Single-Crystalline GaN Nanowires

**Byeongchul Ha,[†] Sung Ho Seo,[†] Jung Hee Cho,[†] Chong S. Yoon,[‡] Jinkyoung Yoo,[§] Gyu-Chul Yi,[§] Chong Yun Park,[||] and Cheol Jin Lee*[,†]**

*Department of Nanotechnology, Hanyang University, Seoul 133-791, Korea, Division of Advanced Materials Science and Engineering, Hanyang University, Seoul 133-791, Korea, Department of Materials Science and Engineering, Pohang University of Science and Technology (POSTECH), San-31 Hyoja-dong, Pohang 790-784, Korea, and Department of Physics, Center for Nanotubes and Nanostructured Composites, Sungkyunkwan University, Suwon 440-746, Korea*

*Received: December 12, 2004; In Final Form: March 21, 2005*

Thin high-quality gallium nitride (GaN) nanowires were synthesized by a catalytic chemical vapor deposition method. The synthesized GaN nanowires with hexagonal single-crystalline structure had thin diameters of 10−50 nm and lengths of tens of micrometers. The thin GaN nanowires revealed UV bands at 3.481 and 3.285 eV in low-temperature PL measurements due to the recombination of donor-bound excitons and donor−acceptor pairs, respectively. The blue shifts of UV bands in the low-temperature PL measurement were observed, indicating quantum confinement effects in the thin GaN nanowires which have smaller diameters than the exciton Bohr radius, 11 nm. For field emission properties of GaN nanowires, the turn-on field of GaN nanowires was 8.5 V/$\mu$m and the current density was about 0.2 mA/cm$^2$ at 17.5 V/$\mu$m, which is sufficient for the applications of field emission displays and vacuum microelectronic devices. Moreover, the GaN nanowires indicated stronger emission stability compared with carbon nanotubes.

### 1. Introduction

Synthesis of gallium nitride (GaN) nanowires has attracted much attention because of their one-dimensional distinctive optical, electrical, and magnetic nanostructure properties.[1−8] Many research groups have studied the synthesis of GaN nanowires using various methods such as laser ablation, pyrolysis, and catalytic chemical vapor deposition (CCVD).[9−12] GaN is an important semiconductor material with a wide direct band gap (3.4 eV) because of its various applications in blue and ultraviolet light emission, high-temperature electronic devices, and high-power electronic devices. Recently, GaN nanowires promised bright hope for use as sensors, electronic devices, logic gates, light-emitting diodes, and diode lasers.[1−7]

To apply the GaN nanowires to various areas, several research groups have studied optical properties such as Raman and photoluminescence (PL). There have been a few reports about room-temperature PL measurements of GaN nanowires. However, most room-temperature PL measurements performed on the GaN nanowires revealed no quantum confinement effect, showing red shifts because most GaN-nanowire diameters were larger than the GaN excitonic Bohr radius, $a_B$, 11 nm.[13,14] Only Chen et al. reported a blue shift in the band edge emission peak from GaN nanowires with 10−40 nm diameters at room-temperature PL measurements, indicating that some parts of GaN nanowires have smaller diameters than the excitonic Bohr radius of GaN, 11 nm.[15] However, there was no report showing blue shift in low-temperature PL from thin GaN nanowires which have smaller diameters than the Bohr radius, 11 nm. Low-temperature PL measurements present more precise spectroscopic information than room-temperature PL measurements by reducing thermally activated nonradioactive recombination processes and thermal line broadening. The PL peak shifts of 80 and 54 meV were reported in the temperature range of 10−340 K for bulk GaN and GaN quantum dots, respectively.[16] The main reduction of the band gap at high-temperature originates from interaction with LO phonons, resulting in the red shift of the band gap.[16,17] Therefore, we performed low-temperature PL measurements to investigate the exact relation with the quantum confinement effect on the size effect from the thin GaN nanowires with 10−50 nm diameters without reflecting on the temperature effect. We previously reported the synthesis of GaN nanowires by a thermal CCVD method using a mixture source of Ga and GaN powder.[11] However, in this work differently from the previous work, we used only Ga powder as a Ga source and separated a Ga source from a substrate about 10 mm.

Even though the optical and electrical properties of GaN materials were announced by many research groups, there have been rare reports for field emission from GaN materials.[18−24] Berishev et al.[18] and Sugino et al.[19] investigated the electron field emission from GaN films. Ward et al. reported the field emission from GaN pyramid arrays for the high-power and high-temperature microelectronic devices.[20] They reported that the

* To whom correspondence should be addressed. Tel: +82-2-2293-4744. Fax: +82-2-2220-0768. E-mail: cjlee@hanyang.ac.kr.
[†] Department of Nanotechnology, Hanyang University.
[‡] Division of Advanced Materials Science Engineering, Hanyang University.
[§] Pohang University of Science and Technology.
[||] Sungkyunkwan University.

10.1021/jp044334c CCC: $30.25 
Published on Web 05/12/2005

pyramid or roughing shapes of GaN increase the field enhancement factor ($\beta$), lowering anode voltage for the electron emission.[19,20] Thus, further enhancement of field emission characteristics is anticipated by the one-dimensional structures of nanowires. Recently, the field emission from GaN nanowires or nanorods was reported.[21−24] However, further study of the field emission from thin GaN nanowires was still necessary. In this work, we demonstrated the synthesis of high-quality GaN nanowires with small diameter and their structural properties, and we also studied optical and field emission properties from the thin GaN nanowires.

## 2. Experimental Section

GaN nanowires were synthesized by CCVD. The nickel nitrate/ethanol solution with the concentration of 0.01 M was dropped on the surface of the alumina ($Al_2O_3$) substrates (10 × 10 mm in size). After drying the substrate at 400 °C in air, the catalyzed alumina substrates were placed vertically on the side of a quartz boat loaded with the Ga powder (Ga: 99.999%, Sigma-Aldrich). The upright distance between the Ga source and the Ni-catalyzed alumina substrate was about 10 mm. The quartz boat containing the Ga source and the catalyzed alumina substrate were placed inside a quartz tube at the center of a reactor. The quartz tube was evacuated to less than 0.01 Torr. A carrier gas of argon was kept flowing through the quartz tube at a flow rate of 1000 sccm. Meanwhile, the temperature was increased from room temperature to 900−1000 °C at a rate of 35 °C/min. The GaN nanowires were synthesized in the temperature range of 900−1000 °C for 10−30 min under a constant flow of 100 sccm ammonia ($NH_3$) and 300 sccm hydrogen ($H_2$). After the reactions, light yellow-colored materials were deposited on the surface of the alumina substrate. The morphologies and microstructures of the deposited GaN nanowires were investigated by scanning electron microscopy (SEM) [Hitachi S-4700], transmission electron microscopy (TEM) [Hitachi H-9000 NAR], X-ray diffraction (XRD) [Rigaku DMAX PSPC MDG 2000], energy-dispersive X-ray spectroscopy (EDX) [Hitachi S-4700], Raman spectroscopy using the 514.5- nm line of an $Ar^+$ laser with a power of 20 mW, and photoluminescence (PL) measurements using the excitation source of 325-nm line of a He−Cd laser.

To measure field emission from the GaN nanowires, the GaN nanowires grown on alumina substrates were dipped in ethanol solution, and performed sonication to separate nanowires from the alumina substrate. Then, the suspension which contained GaN nanowires was dropped on the Ti(1000 Å)/Si substrate several times. The substrate was dried in air, followed by baking at 400 °C for 20 min using a rapid thermal annealing in argon ambient to remove the ethanol and maintain good adhesion between nanowires and the substrate. Field electron emission measurements were performed in a vacuum chamber at a pressure of less than $5 \times 10^{-6}$ Torr. The cathode consisted of Ti film deposited on the silicon substrate and the anode was a copper plate. The distance between the cathode and the anode was about 200 $\mu$m, and the measured emission area was 5 mm$^2$. Emission current was monitored with a Keithley 6517 A and recorded at intervals of 0.5 s.

## 3. Results and Discussion

SEM observation shows that the synthesized GaN nanowires have diameters ranging from 10 to 50 nm and lengths of several tens of micrometers, as shown in Figure 1. The as-synthesized GaN nanowires have uniform diameters over the length without amorphous material deposition. The inset of Figure 1 indicates

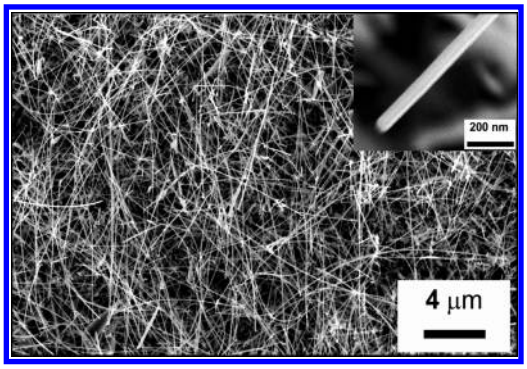


**Figure 1.** SEM micrographs of GaN nanowires on alumina substrates.

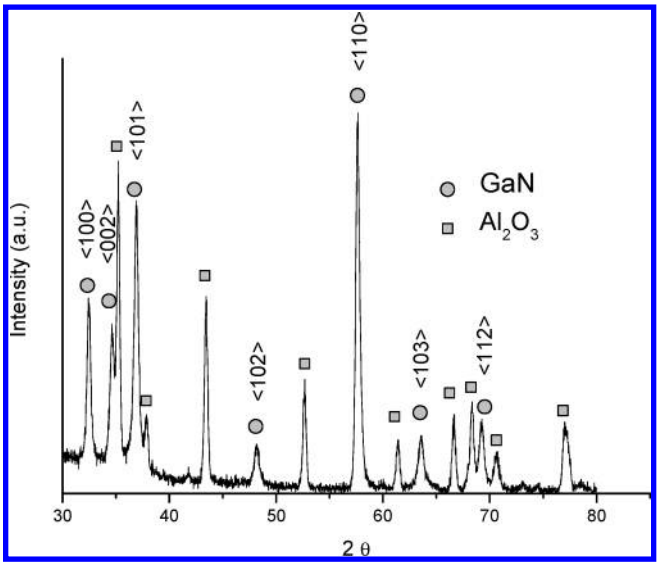


**Figure 2.** XRD diffraction patterns of GaN nanowires on alumina substrates. The high intensities of GaN diffraction peaks at (110). X-ray diffraction (XRD) spectrum shows the peaks of (100), (002), (101), (102), (110), (103), and (112), identifying the GaN nanowires as hexagonal wurtzite structures with lattice parameters $a = 3.189$ Å and $c = 5.185$ Å. The other peaks are identified as the rhombohedral $Al_2O_3$ substrate with lattice parameters $a = 4.760$ Å and $c = 12.997$ Å.

a straight GaN nanowire tip with clean and uniform diameter. It was confirmed through EDX analysis that the synthesized nanowires are GaN nanowires, consisting of gallium (Ga) and nitrogen (N) elements. In this work, we used a high flow rate of hydrogen gas to synthesize GaN nanowires. We consider that hydrogen plays a key role to obtain thin high-purity GaN nanowires because hydrogen passivation on the surface of a GaN nanowire induces surface stabilization, reducing oxygen adsorption and lessening surface roughness.[6,24]

The GaN nanowires were characterized with Cu Kα radiation by an X-ray diffractometer. In Figure 2, an XRD spectrum shows peaks of (100), (002), (101), (102), (110), (103), and (112), indicating that the GaN nanowires have hexagonal wurtzite structures with lattice parameters $a = 3.189$ Å and $c = 5.185$ Å. The other peaks are identified as the rhombohedral $Al_2O_3$ substrate with lattice parameters $a = 4.760$ Å and $c = 12.997$ Å. The XRD results reveal that the synthesized GaN nanowires have highly crystalline structure. The relatively dominant (101) and (110) peaks of the GaN nanowires imply that most of the GaN nanowires are aligned toward (101) and (110) directions.

TEM shows that the as-synthesized GaN nanowires have no dislocations or stacking faults, revealing high-quality nanowires as shown in Figure 3. It is hard to observe any defects and amorphous sheath on the surface of the GaN nanowires. The

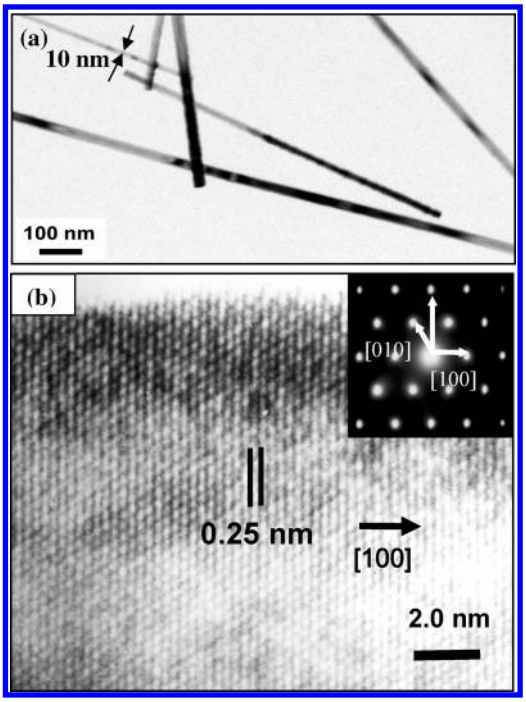


**Figure 3.** TEM micrographs of GaN single-crystal nanowires: (a) low-resolution TEM image of GaN nanowires; (b) high-resolution TEM images of a GaN nanowire with [100] axis growth direction. Inset: Selected area electron diffraction of a single GaN nanowire, indicating a single-crystalline structure of a GaN nanowire.

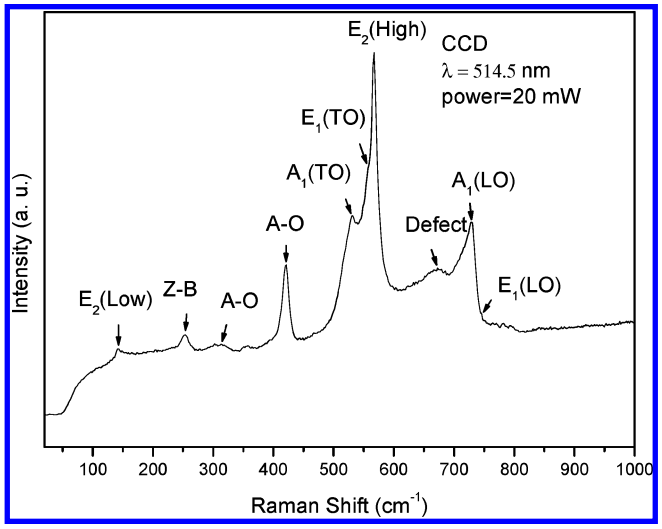


**Figure 4.** Raman spectra of GaN nanowires: Z-B: zone-boundary phonon, A-C: acoust-overtone. $E_2$(Low), $A_1$(TO), $E_1$(TO), $E_2$(High), $A_1$(LO), and $E_1$(LO): first-order Raman modes.

lattice spacing of the GaN nanowires is estimated to be 0.25 nm from the clear lattice fringes of the TEM image. TEM observation confirms that the as-synthesized GaN nanowires indicate single-crystalline hexagonal wurtzite structures with [100] direction, consistent with XRD measurement. The selected area electron diffraction (SAED) pattern indicates that the GaN nanowires grow along the [100] direction and have single-crystalline structures.

Raman spectra for the GaN nanowires are shown in Figure 4. These spectra clearly indicate that Raman peaks appear at 143, 254, 315, 421, 532, 559, 567, 673, 729, and 745 $cm^{-1}$. Table 1 shows the Raman peaks and the related symmetry assignments from both GaN film and GaN nanowires. GaN nanowires indicate first-order Raman modes at 143, 532, 559, 567, 729, and 745 $cm^{-1}$ and second-order Raman phonon modes

**TABLE 1: Raman Peaks in the GaN Film and GaN Nanowires and the Related Symmetry Assignments**

| GaN films[a] ($cm^{-1}$) | GaN NWs[b] ($cm^{-1}$) | GaN NWs[a] ($cm^{-1}$) | this work ($cm^{-1}$) | symmetry assignment |
|---|---|---|---|---|
| 145 | | 143 | 143 | $E_2$(Low), first-order |
| | | 254 | 254 | zone-boundary phonon |
| | | 314 | 315 | acoust, overtone[c] |
| | 420 | 420 | 421 | acoust, overtone[c] |
| 533 | 531 | 531 | 532 | $A_1$(TO), first-order |
| 561 | 560 | 559 | 559 | $E_1$(TO), first-order |
| 571 | 569 | 567 | 567 | $E_2$(High), first-order |
| | | 670 | 673 | defect related phonon |
| 737 | 733 | 728 | 729 | $A_1$(LO), first-order |
| 742 | 745 | | 745 | $E_1$(LO), first-order |

[a] Ref 21. [b] Ref 24. [c] Ref 25.

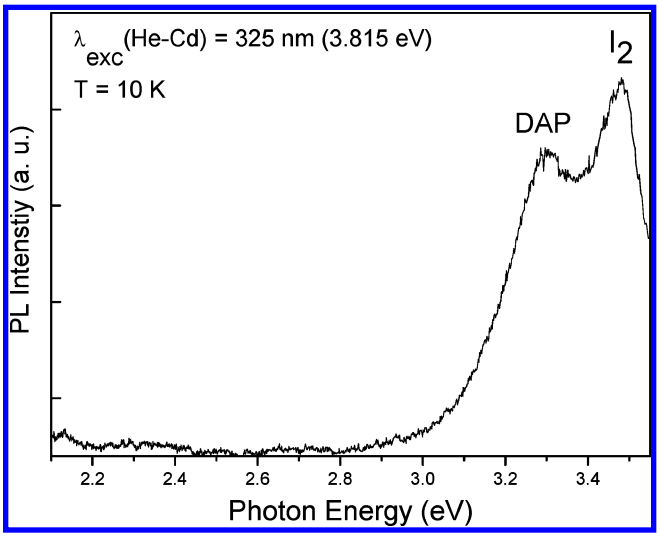


**Figure 5.** Photoluminescence spectra of GaN nanowires measured at 10 K under excitation at 325 nm. The peaks at 3.481 and 3.285 eV are attributed to the $I_2$ line as the donor-bound exciton transition and the donor−acceptor pair (DAP) line, respectively.

at 254, 315, 421, and 673 $cm^{-1}$ activated by the finite-size effects. The peaks at 143, 532, 559, 567, 729, and 745 $cm^{-1}$ agree with the phonon vibration frequencies of $E_2$(Low), $A_1$(TO), $E_1$(TO), $E_2$(High), $A_1$(LO), and $E_1$(LO) modes of the hexagonal wurtzite GaN, respectively. These first-order Raman modes are associated with the group-theoretical symmetry selection rule for the wurtzite crystal: that is, the $C_{6v}$ symmetry group. Compared with GaN films, the broadening and the lower-frequency shifts of the first-order modes are attributed to phonon confinement due to the nanodimensional systems.[26] Our results agree well with previous results reported by Liu et al. with the exception of the $E_1$(LO) mode.[26] $E_1$(LO) and $A_1$(LO) modes are associated with interaction with LO phonons at high temperature, resulting in the red shift of the band gap.[16,17] The modes at 315 and 421 $cm^{-1}$ are characteristics of an acoustic phonon overtone, and the mode at 254 $cm^{-1}$ is characteristic of zone-boundary phonons activated by surface disorders and finite-size effects.[26] The mode at 673 $cm^{-1}$ is a feature of a defect-related phonon. The small defect mode contributes to minimizing defect-related PL peak shifts. Raman spectra indicate that the synthesized GaN nanowires have high-crystalline structures, supporting TEM and XRD measurements.

A PL spectrum was obtained at 10 K using a He−Cd laser with excitation at 325 nm as shown in Figure 5. The high-crystalline structure and low-temperature PL measurements of the synthesized GaN nanowires contribute to minimizing the defect-related and temperature-related PL peak shifts, respec-

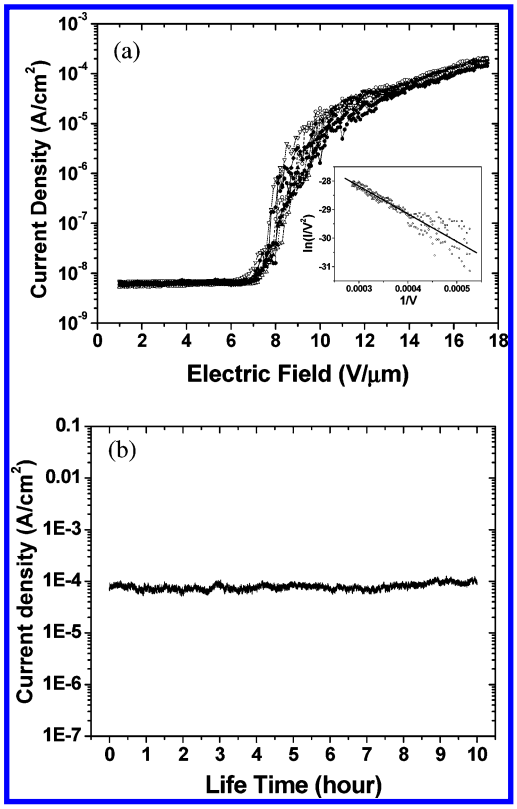


**Figure 6.** (a) Emission current densities from GaN nanowires positioned on a Ti/Si substrate. The inset shows the corresponding Fowler−Nordheim plots. (b) The lifetime measurements of field emission from GaN nanowires.

tively. Low-temperature PL indicates that the $I_2$ line at 3.481 eV leads to a near band-edge transition, that is, band-to-band recombination of free excitons bound to neutral donors. The $I_2$ band has an asymmetrical broad line shape due to the one-dimensional nanosize structure of GaN nanowires. The blue shift of the ultraviolet band is 9 meV, in contrast with the 3.472 eV of the $I_2$ lines of the GaN bulk.[27] We believe that the blue shift of the $I_2$ line originated from a quantum confinement effect because some of the GaN nanowires have diameters less than the Bohr exciton radius of GaN, 11 nm, as shown in Figure 3a.[28,29] The blue shift of the $I_2$ line of GaN nanowires is revealed only at the diameter sizes below the exciton Bohr radius (11 nm).[29,30] On the contrary, the blue shift of the $I_2$ line is not exhibited with much larger diameters than the exciton Bohr radius, 11 nm.[28,31] Thus, it is considered that the quantum confinement effect originates from the GaN nanowires which have smaller diameters than the exciton Bohr radius of the GaN, 11 nm. The blue shift of the $I_2$ line implies that the band gap of GaN nanowires increases with the decreasing diameters. The band at 3.285 eV is characterized by the zero phonon line (ZPL) for the recombination process associated with donor−acceptor pairs (DAP). The blue shift of the DAP band is 15 meV, in contrast with the 3.27 eV of the DAP line of the GaN bulk.[27,32] The synthesized GaN nanowires have the relatively weak yellow band emission of about 2.2 eV, indicating high-purity nanowires associated with minute nitrogen vacancies and surface structural defects, supporting a Raman analysis.[33,34]

The field emission characteristics are shown in Figure 6. A typical turn-on field, which produces the current density of 0.1 $\mu$A/cm$^2$, is about 8.5 V/$\mu$m. This turn-on field is much lower than about that of GaN thin films,[18] but much higher than that of CNTs.[35] The emission current density reaches about 0.2 mA/cm$^2$ at an applied field of about 17.5 V/$\mu$m, indicating relatively lower emission current density than the previously reported value of ZnO.[36] The Fowler−Nordheim (FN) plot was shown in the inset of Figure 6. To calculate the field enhancement factor ($\beta$), we used the Fowler−Nordheim (FN) equation:

$$J = A(\beta^2V^2/\phi d^2)\exp(-B\phi^{3/2}d/\beta V)$$

where $J$ is the current density, $A = 4.43 \times 10^{-22}$ ($AV^{-2}$ eV), $B = 6.83 \times 10^9$ ($VeV^{-3/2}$ V m$^{-1}$), $\beta$ is a field enhancement factor, $\phi$ is the work function, $d$ is a distance between the anode and the cathode, and $V$ is the applied voltage. When assuming the work function to be 4.1 eV, the field enhancement factor $\beta$ is estimated to be 1170, the value of which is sufficient for the applications of field emission displays. We also investigated the stability of field emission properties through the lifetime measurements for GaN nanowires. The GaN nanowires indicate very stable emission current densities of 7.91 $\mu$A/cm$^2$ with 8.7% current density fluctuation for 10 h without any degradation, as shown in Figure 6b. Compared with the previously reported emission stability of the carbon nanotubes, the emission stability of the GaN nanowires is much better than that of single-walled carbon nanotubes.[39] We consider that the stable emission properties were caused by good crystallinity and high oxidation durability of the GaN nanowires. Therefore, we suggest that GaN nanowires can be used as stable field emitters for field emission displays.

## 4. Conclusions

We demonstrated the synthesis of thin single-crystalline GaN nanowires and their optical and field emission properties. The synthesized GaN nanowires were shown to be single-crystalline wurtzite structures. Raman spectra indicate that the synthesized GaN nanowires have high-crystalline structure, showing a small defect mode. The intense UV luminescence due to the recombination of an exciton bound to a neutral donor ($I_2$) and donor−acceptor pairs (DAP) was shown at low-temperature PL measurements. We suggest that the blue shifts of UV bands indicate quantum confinement effects from PL measurement in thin GaN nanowires. We confirm that the blue shifts of UV bands in PL originated from the thin GaN nanowires which have smaller diameters than the exciton Bohr radius, 11 nm. The thin GaN nanowires also demonstrated fairly good field emission characteristics and strong emission stability, showing possible applications to field emission displays and vacuum microelectronic devices.

**Acknowledgment.** This work was supported by the Center for Nanotubes and Nanostructured Composites at Sungkyunkwan University and by the National R&D project for Nano Science and Technology of MOST.

## References and Notes

(1) Duan, X.; Niu, C.; Sahi, V.; Chen, J.; Wallace Parce, J.; Empedocles, S.; Goldman, J. L. *Nature* **2003**, *425*, 274.
(2) Yang, P. *Nature* **2003**, *425*, 243.
(3) Whang, D.; Jin, S.; Wu, Y.; Lieber, C. M. *Nano Lett.* **2003**, *3*, 1255.
(4) Choi, H.-J.; Johnson, J. C.; He, R.; Lee, S.-K.; Kim, F.; Pauzauskie, P.; Goldberger, J.; Saykally, R. J.; Yang, P. *J. Phys. Chem. B* **2003**, *107*, 8721.
(5) McAlpine, M. C.; Friedman, R. S.; Jin, S.; Lin, K.-H.; Wang, W. U.; Lieber, C. M. *Nano Lett.* **2003**, *3*, 1531.
(6) Kim, J.-R.; Kim, H. M.; Park, J. W.; Kim. J.-J.; Kim, J.; Lee, C. J.; Lyu, S. C. *Appl. Phys. Lett.* **2002**, *80*, 3548.
(7) Kim, J.-R.; Kim, B.-K.; Lee, I. J.; Kim, J.-J.; Kim, J.; Lyu, S. C.; Lee, C. J. *Phys. Rev. B* **2004**, *69*, 233303.
(8) Deepak, F. L.; Govindaraj, P. V.; Govindaraj, A.; Rao, C. N. R. *Chem. Phys. Lett.* **2003**, *374*, 314.

(9) Duan, X.; Lieber, C. M. *J. Am. Chem. Soc.* **2000**, *22*, 188.
(10) Han, W.-Q.; Zettl, A. *Appl. Phys. Lett.* **2002**, *80*, 303.
(11) Lyu, S. C.; Cha, O. H.; Suh, E.-K.; Ruh, H.; Lee, H. J.; Lee, C. J. *Chem. Phys. Lett.* **2003**, *367*, 136.
(12) Wang, J. C.; Feng, S. Q.; Yu, D. P. *Appl. Phys. A* **2002**, *75*, 691.
(13) Chang, K.-W.; Wu, J.-J. *J. Phys. Chem. B* **2002**, *106*, 7796.
(14) Zhang, J.; Zhang, L. D.; Wang, X. F.; Liang, C. H.; Peng, X. S.; Wang, Y. W. *J. Chem. Phys.* **2001**, *115*, 5714.
(15) Chen, X.; Li, J.; Cao, Y.; Lan, Y.; Li, H.; He, M.; Wang, C.; Zhang, Z.; Qiao, Z. *Adv. Mater.* **2000**, *12*, 1432.
(16) Ramvall, P.; Tanaka, S.; Nomura, S.; Riblet, P.; Aoyagi, Y. *Appl. Phys. Lett.* **1999**, *75*, 1935.
(17) Sheih, S. J.; Tsen, K. T.; Ferry, D. K.; Botchkarev, A.; Sverdlov, B.; Salvador, A.; Morkoç, H. *Appl. Phys. Lett.* **1995**, *67*, 1757.
(18) Berishev, I.; Bensaoula, A.; Rusakova, I.; Karabutov, A.; Ugarov, M.; Ageev, V. P. *Appl. Phys. Lett.* **1998**, *73*, 1808.
(19) Sugino, T.; Hori, T.; Kimura, C.; Yamamoto, T. *Appl. Phys. Lett.* **2001**, *78*, 3229.
(20) Ward, B. L.; Nam, O.-H.; Hartman, J. D.; English, S. L.; McCarson, B. L.; Schlesser, R.; Sitar, Z.; Davis, R. F.; Nemanich, R. J. *J. Appl. Phys.* **1998**, *84*, 5238.
(21) Chen, C.-C.; Yeh, C.-C.; Chen, C. H.; Yu, M.-Y., Liu, H.-L.; Wu, J.-J.; Chen, K. H.; Chen, K. C.; Peng, J.-Y.; Chen, Y.-F. *J. Am. Chem. Soc.* **2001**, *123*, 2791.
(22) Kim, H.-W.; Kang, T. W.; Chung, K. S.; Hong, J. P.; Choi, W. B. *Chem. Phys. Lett.* **2003**, *377*, 491.
(23) Kim, T. Y.; Lee, S. H.; Mo, Y. H.; Shim, H. W.; Nahm, K. S.; Suh, E.-K.; Yang, J. W.; Lim, K.; Park, G. S. *J. Cryst. Growth* **2003**, *257*, 97.
(24) Wu, Y.; Cui, Y.; Huynh, L.; Barrelet, C. J.; Bell, D. C.; Lieber, C. M. *Nano Lett.* **2004**, *4*, 433.
(25) Siegle, H.; Kaczmarczyk, G.; Filippidis, L.; Litvinchuk, A. P.; Hoffmann, A.; Thomsen, C. *Phys. Rev. B* **2000**, *61*, 6720.
(26) Liu, H.-L.; Chen, C.-C.; Chia, C.-T.; Yeh, C.-C.; Chen, C.-H.; Yu, M.-Y.; Keller, S.; DenBaars, S. P. *Chem. Phys. Lett.* **2001**, *345*, 245.
(27) Glaser, E. R.; Kennedy, T. A.; Doverspike, K.; Rowland, L. B.; Gaskill, D. K.; Freitas, J. A., Jr.; Khan, M. A.; Olson, D. T.; Kuznia, J. N.; Wickenden, D. K. *Phys. Rev. B* **1995**, *51*, 13326.
(28) Chen, X.; Xu, J.; Wang, R. M.; Yu, D. *Adv. Mater.* **2003**, *15*, 419.
(29) Xie, Y.; Qian, Y.; Wang, W. *Science* **1996**, *272*, 1926.
(30) Preschilla, N.; Major, S.; Kumar, N. *Appl. Phys. Lett.* **2000**, *77*, 1861.
(31) Yoon, J.-W.; Sasaki, T.; Roh, C. H.; Shim, S. H.; Shim, K. B.; Koshizaki, N. *Thin Solid Films* **2005**, *471*, 273.
(32) Rhee, S. J.; Kim, S.; Reuter, E. E.; Bishop, S. G. *Appl. Phys. Lett.* **1998**, *73*, 2636.
(33) Look, D. C.; Farlow, G. C.; Drevinsky, P. J.; Bliss, D. F.; Sizelove, J. R. *Appl. Phys. Lett.* **2003**, *83*, 3525.
(34) Hofmann, D. M.; Kovalev, D.; Steude, G.; Meyer, B. K.; Hoffmann, A.; Eckey, L.; Heitz, R.; Detchprom, T.; Amano, H.; Akasaki, I. *Phys. Rev. B* **1995**, *52*, 16702.
(35) Cheng, Y.; Zhou, O. *C. R. Physique* **2003**, *4*, 1021.
(36) Lee, C. J.; Lee, T. J.; Lyu, S. C.; Zhang, Y.; Ruh, H.; Lee, H. J. *Appl. Phys. Lett.* **2002**, *81*, 3648.
(37) Sveningsson, M.; Morjan, R.-E.; Nerushev, O. A.; Sato, Y.; Bäckström, J.; Campbell, E. E. B.; Rohmund, F. *Appl. Phys. A* **2001**, *73*, 409.
(38) Wen, J. G.; Lao, J. Y.; Wang, D. Z.; Kyaw, T. M.; Foo, Y. L.; Ren, Z. F. *Chem. Phys. Lett.* **2003**, *372*, 717.
(39) Bonard, J.-M.; Salvetat, J.-P.; Stöckli, T.; de Heer, W. A.; Forró, L.; Châtelain, A. *Appl. Phys. Lett.* **1998**, *73*, 918.